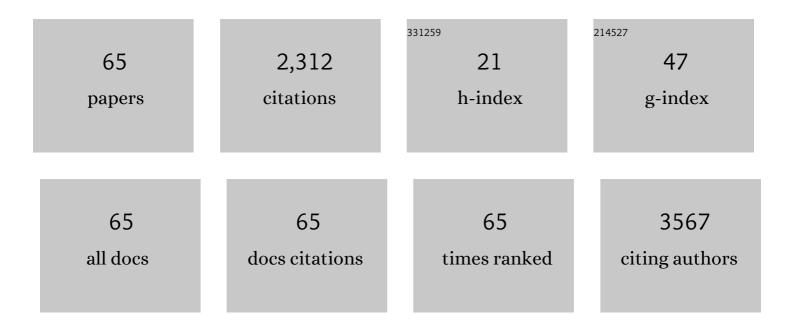
List of Publications by Year in descending order

Source: https://exaly.com/author-pdf/6567771/publications.pdf Version: 2024-02-01



#	Article	IF	CITATIONS
1	A new class of doped nanobulk high-figure-of-merit thermoelectrics by scalable bottom-up assembly. Nature Materials, 2012, 11, 233-240.	13.3	462
2	Al-Doped Zinc Oxide Nanocomposites with Enhanced Thermoelectric Properties. Nano Letters, 2011, 11, 4337-4342.	4.5	405
3	Bonding-induced thermal conductance enhancement at inorganic heterointerfaces usingÂnanomolecular monolayers. Nature Materials, 2013, 12, 118-122.	13.3	223
4	High Electrical Conductivity Antimony Selenide Nanocrystals and Assemblies. Nano Letters, 2010, 10, 4417-4422.	4.5	87
5	Seebeck and Figure of Merit Enhancement in Nanostructured Antimony Telluride by Antisite Defect Suppression through Sulfur Doping. Nano Letters, 2012, 12, 4523-4529.	4.5	80
6	Nanowire-filled polymer composites with ultrahigh thermal conductivity. Applied Physics Letters, 2013, 102, .	1.5	74
7	Seebeck Tuning in Chalcogenide Nanoplate Assemblies by Nanoscale Heterostructuring. ACS Nano, 2010, 4, 5055-5060.	7.3	65
8	Heavy element doping for enhancing thermoelectric properties of nanostructured zinc oxide. RSC Advances, 2014, 4, 6363.	1.7	61
9	Multifold improvement of thermoelectric power factor by tuning bismuth and antimony in nanostructured n-type bismuth antimony telluride thin films. Materials and Design, 2019, 163, 107549.	3.3	61
10	Structurally stabilized olivine lithium phosphate cathodes with enhanced electrochemical properties through Fe doping. Energy and Environmental Science, 2011, 4, 4978.	15.6	59
11	A microprobe technique for simultaneously measuring thermal conductivity and Seebeck coefficient of thin films. Applied Physics Letters, 2010, 96, .	1.5	55
12	Harnessing Topological Band Effects in Bismuth Telluride Selenide for Large Enhancements in Thermoelectric Properties through Isovalent Doping. Advanced Materials, 2016, 28, 6436-6441.	11.1	44
13	Microsphere Bouquets of Bismuth Telluride Nanoplates: Room-Temperature Synthesis and Thermoelectric Properties. Journal of Physical Chemistry C, 2010, 114, 1796-1799.	1.5	36
14	Nanoscale Heterostructures with Molecular-Scale Single-Crystal Metal Wires. Journal of the American Chemical Society, 2010, 132, 20-21.	6.6	34
15	Multifold Increases in Thermal Conductivity of Polymer Nanocomposites through Microwave Welding of Metal Nanowire Fillers. Advanced Materials Interfaces, 2015, 2, 1500186.	1.9	33
16	A noncontact thermal microprobe for local thermal conductivity measurement. Review of Scientific Instruments, 2011, 82, 024902.	0.6	32
17	Lattice thermal conductivity diminution and high thermoelectric power factor retention in nanoporous macroassemblies of sulfur-doped bismuth telluride nanocrystals. Applied Physics Letters, 2012, 100, .	1.5	32
18	Microwave synthesis of branched silver nanowires and their use as fillers for high thermal conductivity polymer composites. Nanotechnology, 2016, 27, 175601.	1.3	32

#	Article	IF	CITATIONS
19	Surface diffusion driven nanoshell formation by controlled sintering of mesoporous nanoparticle aggregates. Nanoscale, 2010, 2, 1423.	2.8	25
20	Pressure-induced insulator-to-metal transitions for enhancing thermoelectric power factor in bismuth telluride-based alloys. Physical Chemistry Chemical Physics, 2017, 19, 12784-12793.	1.3	23
21	Multifold enhancements in thermoelectric power factor in isovalent sulfur doped bismuth antimony telluride films. Materials Research Bulletin, 2021, 142, 111426.	2.7	23
22	Branched titania nanotubes through anodization voltage control. Thin Solid Films, 2011, 520, 235-238.	0.8	19
23	Kinetics of titania nanotube formation by anodization of titanium films. Thin Solid Films, 2011, 519, 1821-1824.	0.8	19
24	Tailoring Electrical Transport Across Metal–Thermoelectric Interfaces Using a Nanomolecular Monolayer. ACS Applied Materials & Interfaces, 2016, 8, 4275-4279.	4.0	19
25	Synthesis and Thermoelectric Properties of Thin Film Assemblies of Bismuth Telluride Nanopolyhedra. Chemistry of Materials, 2011, 23, 3029-3031.	3.2	18
26	Metalâ^'Dielectric Interface Toughening by Catalyzed Ring Opening in a Monolayer. Journal of Physical Chemistry Letters, 2010, 1, 336-340.	2.1	15
27	Gold-titania interface toughening and thermal conductance enhancement using an organophosphonate nanolayer. Applied Physics Letters, 2013, 102, 201605.	1.5	15
28	Interface engineering through atomic dopants in HfO2-based gate stacks. Journal of Applied Physics, 2013, 114, .	1.1	14
29	Threshold conductivity switching in sulfurized antimony selenide nanowires. Applied Physics Letters, 2011, 99, .	1.5	13
30	Civil Society-Driven Drug Policy Reform for Health and Human Welfare—India. Journal of Pain and Symptom Management, 2017, 53, 518-532.	0.6	13
31	Multifold Electrical Conductance Enhancements at Metal–Bismuth Telluride Interfaces Modified Using an Organosilane Monolayer. ACS Applied Materials & Interfaces, 2017, 9, 2001-2005.	4.0	13
32	Work function tuning at Au-HfO2 interfaces using organophosphonate monolayers. Applied Physics Letters, 2016, 108, .	1.5	11
33	Divalent doping-induced thermoelectric power factor increase in p-type Bi2Te3 via electronic structure tuning. Journal of Applied Physics, 2019, 125, .	1.1	11
34	Ring-Opening-Induced Toughening of a Low-Permittivity Polymerâ^'Metal Interface. ACS Applied Materials & Interfaces, 2010, 2, 1275-1280.	4.0	10
35	Tuning of noble metal work function with organophosphonate nanolayers. Applied Physics Letters, 2014, 105, .	1.5	10
36	Multifold Seebeck increase in RuO2 films by quantum-guided lanthanide dilute alloying. Applied Physics Letters, 2014, 104, 053903.	1.5	10

#	Article	IF	CITATIONS
37	Metal–dielectric interface toughening by molecular nanolayer decomposition. Journal of Applied Physics, 2010, 108, 034317.	1.1	9
38	Selective Deposition of a Cross-Linked Low-Permittivity Polycarbosilane on Copper. ACS Applied Materials & Interfaces, 2010, 2, 2180-2184.	4.0	9
39	Branched Copper Nanocrystal Corals by Room-Temperature Galvanic Displacement. Crystal Growth and Design, 2010, 10, 3925-3928.	1.4	9
40	Engineering Faceted Nanoporosity by Reactions in Thin-Film Oxide Multilayers in Crystallographically Layered Calcium Cobaltate for Thermoelectrics. ACS Applied Nano Materials, 2021, 4, 9904-9911.	2.4	9
41	Hydrophobic fluoroalkylsilane nanolayers for inhibiting copper diffusion into silica. Applied Physics Letters, 2010, 96, 143121.	1.5	8
42	Atomistic fracture energy partitioning at a metal-ceramic interface using a nanomolecular monolayer. Physical Review B, 2011, 83, .	1.1	8
43	Atomistic mechanisms of moisture-induced fracture at copper-silica interfaces. Applied Physics Letters, 2011, 99, 133103.	1.5	8
44	Softening in silver-nanowire-filled polydimethylsiloxane nanocomposites. Applied Physics Letters, 2014, 105, 013110.	1.5	8
45	Effects of chemical intermixing on electrical and thermal contact conductances at metallized bismuth and antimony telluride interfaces. Journal of Vacuum Science and Technology A: Vacuum, Surfaces and Films, 2015, 33, .	0.9	8
46	Frequency-tunable toughening in a polymer-metal-ceramic stack using an interfacial molecular nanolayer. Nature Communications, 2018, 9, 5249.	5.8	8
47	Gating heat transport by manipulating convection in a magnetic nanofluid. Applied Physics Letters, 2013, 102, .	1.5	6
48	Environment-dependent interfacial strength using first principles thermodynamics: The example of the Pt-HfO2 interface. Journal of Applied Physics, 2013, 114, 163503.	1.1	6
49	Decreasing friction during Al cold forming using a nanomolecular layer. Journal of Vacuum Science and Technology A: Vacuum, Surfaces and Films, 2017, 35, 020605.	0.9	6
50	Interfacial thermal conductance-rheology nexus in metal-contacted nanocomposites. Applied Physics Letters, 2013, 103, .	1.5	5
51	Enhanced interfacial thermal transport in pnictogen tellurides metallized with a lead-free solder alloy. Journal of Vacuum Science and Technology A: Vacuum, Surfaces and Films, 2015, 33, .	0.9	5
52	Effect of molecular length on the electrical conductance across metal-alkanedithiol-Bi2Te3 interfaces. Applied Physics Letters, 2016, 109, .	1.5	5
53	Interplay between bond breaking and plasticity during fracture at a nanomolecularly-modified metal-ceramic interface. Scripta Materialia, 2016, 121, 42-44.	2.6	5
54	Effect of disordered nanoporosity on electrical and thermal properties of layered Ca3Co4O9 films. Applied Physics Letters, 2022, 120, 061904.	1.5	5

#	Article	IF	CITATIONS
55	Engineering thermoelectric and mechanical properties by nanoporosity in calcium cobaltate films from reactions of Ca(OH) ₂ /Co ₃ O ₄ multilayers. Nanoscale Advances, 2022, 4, 3353-3361.	2.2	5
56	Dye-sensitized solar cells using branched titania nanotube films. Thin Solid Films, 2012, 520, 2764-2768.	0.8	4
57	Factorial toughening at microcorrugated metal-ceramic interfaces. Applied Physics Letters, 2011, 99, 133101.	1.5	3
58	Effects of molecular functionalization sequence on mesoporous silica film properties. Journal of Vacuum Science and Technology B:Nanotechnology and Microelectronics, 2011, 29, 010602.	0.6	3
59	Molecular length effect on work function shifts at copper-organophosphonate-hafnia interfaces. Applied Physics Letters, 2017, 110, .	1.5	3
60	Tailoring Al-SiO2 interfacial work function using an organophosphonate nanolayer. Applied Physics Letters, 2017, 111, .	1.5	3
61	Epitaxial Growth of CaMnO _{3–<i>y</i>} Films on LaAlO ₃ (112Â⁻0) by Pulsed Direct Current Reactive Magnetron Sputtering. Physica Status Solidi - Rapid Research Letters, 2022, 16, .	1.2	3
62	Copper-induced majority charge carrier reversal in bismuth telluride-based nanothermoelectrics. AIP Conference Proceedings, 2019, , .	0.3	2
63	Viscoelastic bandgap in multilayers of inorganic–organic nanolayer interfaces. Scientific Reports, 2022, 12, .	1.6	2
64	Chemical bonding and nanomolecular length effects on work function at Au-organophosphonate-HfO2 interfaces. Applied Physics Letters, 2017, 110, 181604.	1.5	1
65	Experimental Investigation of Magnetically-Induced Thermal Conductance Variations in a Ferromagnetic Nanofluid. , 2011, , .		Ο